Potential for ultrafast dynamic chemical imaging with few-cycle infrared lasers

Toru Morishita[1,2,3]**, Anh-Thu Le**[1]**, Zhangjin Chen**[1]
and C D Lin[1]

[1] J R Macdonald Laboratory, Department of Physics,
Kansas State University, Manhattan, KS, 66506, USA
[2] Department of Applied Physics and Chemistry,
The University of Electro-Communications, 1-5-1 Chofu-ga-oka,
Chofu-shi, Tokyo, 182-8585, Japan
[3] PRESTO, Japan Science and Technology Agency, Kawaguchi,
Saitama 332-0012, Japan
E-mail: cdlin@phys.ksu.edu, toru@pc.uec.ac.jp and atle@phys.ksu.edu

Abstract. We studied the photoelectron spectra generated by an intense few-cycle infrared laser pulse. By focusing on the angular distributions of the *back* rescattered high energy photoelectrons, we show that accurate differential elastic scattering cross-sections of the target ion by *free* electrons can be extracted. Since the incident direction and the energy of the *free* electrons can be easily changed by manipulating the laser's polarization, intensity and wavelength, these extracted elastic scattering cross-sections, in combination with more advanced inversion algorithms, may be used to reconstruct the effective single-scattering potential of the molecule, thus opening up the possibility of using few-cycle infrared lasers as powerful table-top tools for imaging chemical and biological transformations, with the desired unprecedented temporal and spatial resolutions.

IOP Institute of Physics ⟨Φ⟩ DEUTSCHE PHYSIKALISCHE GESELLSCHAFT

Contents

1. Introduction

When an object is illuminated by a plane wave, the amplitude of the diffraction pattern in the far field is the Fourier transform of the object. To achieve high resolution, microscopists use short wavelengths, such as x-rays or high-energy electrons, with energies of tens to hundreds of kilo-electron-volts, to obtain diffraction patterns of the object. For image reconstruction, advanced phase retrieval algorithms have been developed [1, 2].

While these are powerful tools for spatial imaging of structure at the atomic level, they are not adequate for studying chemical and biological transformations that involve complex transient structures [3, 4]. Since these reactions occur within a few to hundreds of femtoseconds, techniques must be developed to observe the coherent atomic motions in the corresponding time scale. As existing x-ray diffractions using light sources from synchrotron radiation have pulse durations of tens of picoseconds, they are not suitable for time resolved imaging. The impending completion of the next generation x-ray free-electron lasers (XFELs) promises to offer extremely short bursts of x-rays with high intensity and duration of several femtoseconds.While these facilities may offer the opportunity to perform time-resolved x-ray diffraction of chemical and biological reactions in the future, they are large and costly facilities. Other ideas and possible new techniques for imaging transient molecules remain highly desirable.

The advent of femtosecond (fs) lasers in the past decades has made it possible to study and control chemical and biochemical reactions.Today laser pulses of duration of a few femtoseconds are widely accessible. However, these infrared lasers have wavelength much longer than the interatomic distances, hence they are considered not suitable for imaging ultrafast structural changes in molecules. To overcome this limitation, an ultrafast electron diffraction (UED) method has been developed [3]–[6] where electron pulses are generated from femtosecond lasers and then accelerated to about 120 keV. These high-energy electrons are then used to image transient molecules. Most recently, UED with temporal resolution of about 100 fs has been used to observe the time-dependent structural change in phase transitions [4].

In this paper, we present a different approach for achieving ultrafast laser induced electron microscopy (LIEM) with infrared lasers. The possibility of using infrared lasers for imaging molecules from laser-induced electron diffraction (LIED) spectra was proposed a decade ago [7]. Clear diffraction minima have been observed in the calculated energy and angle resolved photoelectron spectra for H_2^+ [8] and K_2^+ [9], by solving the time-dependent Schrödinger equation (TDSE) of these molecular ions in the laser field. In LIED, electron
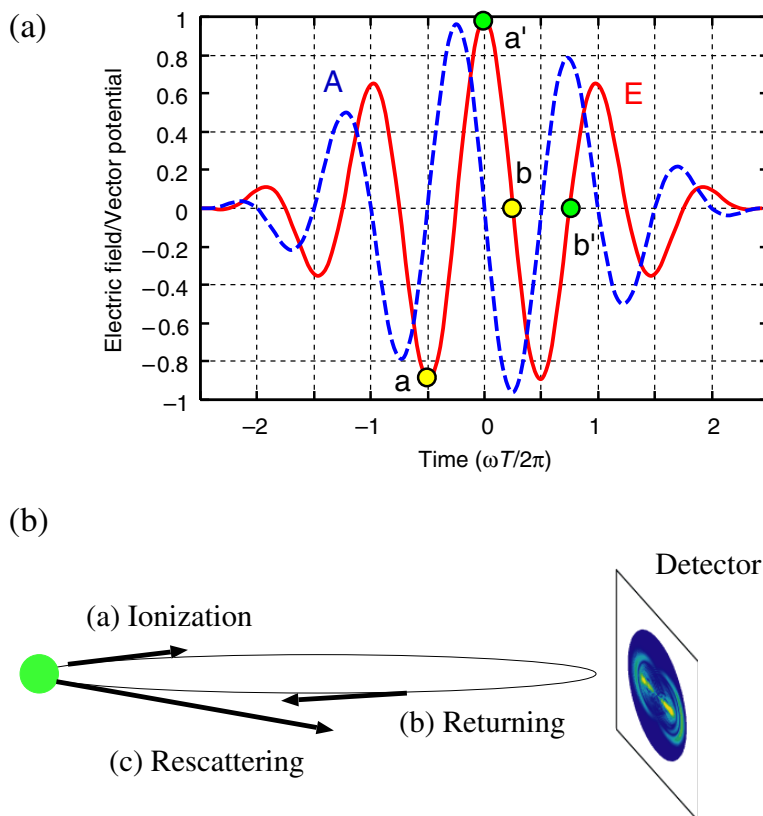
(a)

(b)

Figure 1. (a) The electric field (E) and the vector potential (A) of a typical five-cycle infrared laser pulse. (b) Schematic showing the use of the backward rescattering process to image the molecule by its own electron.

diffraction occurs in the presence of the laser field. To extract structure information, distortions of the diffraction images due to the laser have to be removed and various theoretical methods have been suggested [10, 11]. In the present LIEM, we show that accurate diffraction images by *free* electrons can be extracted from a specific *subset* of laser-induced photoelectron momentum spectra. More precisely, we show that elastic differential cross-sections of the target ion by *free* electrons in the absence of lasers can be extracted from laser-induced momentum spectra, where the temporal resolution is determined by the pulse duration of the laser. Since an infrared laser can be easily manipulated to change its polarization direction, intensity and wavelength, thus a large set of elastic scattering cross-sections can be readily collected. These elastic differential cross-sections can be used to reconstruct the structural information of the molecule after a new inversion algorithm is developed in the future. We comment that conventional diffraction theory cannot be used for retrieving the molecular structure since the electron energies generated by the laser are in the range from several tens to hundreds of electron volts only.

Consider a typical five-cycle laser pulse, with a mean wavelength of 800 nm. The electric field $\vec{E}(t) = -\partial \vec{A}/\partial t$ and the vector potential $\vec{A}(t)$ of such a pulse are depicted in figure 1(a). At time near 'a' where the electric field strength is large, an electron is released by tunneling ionization. Schematically, this electron is first accelerated to the right (figure 1(b)), but it may be driven back in the next half cycle to recollide with the target ion, at time near 'b'. At the

time of recollision near 'b', the returning electrons have energies of about $3.17\,U_P$. Here U_P is the ponderomotive energy, i.e. the mean quiver energy of an electron in a laser field. For electrons that are rescattered into the forward directions (the left-side of figure 1(b)) by the target ion, they will be decelerated by the laser field in the next half cycle and emerge at low energies. These rescattered electrons would carry structural information on the target. However, low-energy electrons on this side are also generated by tunneling ionization near 'a', about half a cycle after 'a'. These electrons would have energies up to about $2\,U_P$, and would interfere with the forward rescattered electrons to damage the diffraction images. On the other hand, electrons that are rescattered into the backward directions will be accelerated by the laser field in the next half cycle and end up at much higher energies of up to about $10\,U_P$ [12]. In LIEM, we analyze only the momentum images of these high-energy electrons that have been rescattered into the backward directions. Their momentum images are not complicated by the laser field, and differential elastic scattering cross-sections of the ion by *free* electrons can be extracted. We note that these high-energy electrons have been observed previously [13]. In the calculated laser-induced electron momentum spectra of H_2^+, clear diffraction minima have also been identified at high energies [8]. These high-energy electrons are well understood as due to backscattering of the returning electrons in the laser field [12]. In this paper, we demonstrate *quantitatively* that it is possible to extract differential elastic scattering cross-sections by *free* electrons from these laser-induced high-energy electrons. The extracted quantities are independent of the lasers and they form the basis of LIEM.

2. Extracting accurate electron scattering cross-sections from laser-induced photoelectron momentum spectra

Accurate high-energy photoelectron momentum spectra of molecules by infrared lasers are not available either experimentally or theoretically so far. For atomic targets, these spectra can be accurately calculated by solving the TDSE.

In figure 2(a), we show the electron momentum images of the simplest atomic hydrogen target generated by a typical infrared laser, chosen for a five-cycle pulse with peak intensity of $5 \times 10^{13}\,\mathrm{W\,cm^{-2}}$ and a mean wavelength of $800\,\mathrm{nm}$. Since the electron yield drops very rapidly with energy (figure 2(c)) the momentum images in figure 2(a) for each photoelectron energy have been renormalized, i.e. the yield integrated along each circle of the p_z–p_x-plane is unity (p_z is along the direction of polarization). We pay attention only to the momentum distributions of high-energy electrons. The images show two clear half circular rings, or ridges, one on the 'left' side with smaller radius, and another on the 'right' with larger radius, where the center of each half circle is shifted from the origin of the p_z–p_x-plane. We call these circular rings back rescattered ridges (BRR), representing electrons that have been rescattered into the backward directions by the target ion. The BRR on the 'right' is from electrons born at time near 'a' (figure 1(a)), travelling to the 'right' by the laser field (figure 1(b)) and then returning to the target ion at time near 'b', where they are rescattered back to the right. Each momentum half circle is represented approximately by $A_r \hat{p}_z + p_o \hat{p}_r$, where the second term represents the momentum vector of the elastically scattered electron with kinetic energy given by $3.17\,U_P = p_0^2/2$, while the first term represents the momentum shift due to the drift of the electron from 'b' where the vector potential is A_r, to the end of the laser pulse. (We used atomic units here where the vector potential has the units of momentum. More precise fitting shows that the shift is $0.95\,A_r$.) Similarly, the BRR on the left is due to electrons that were born near
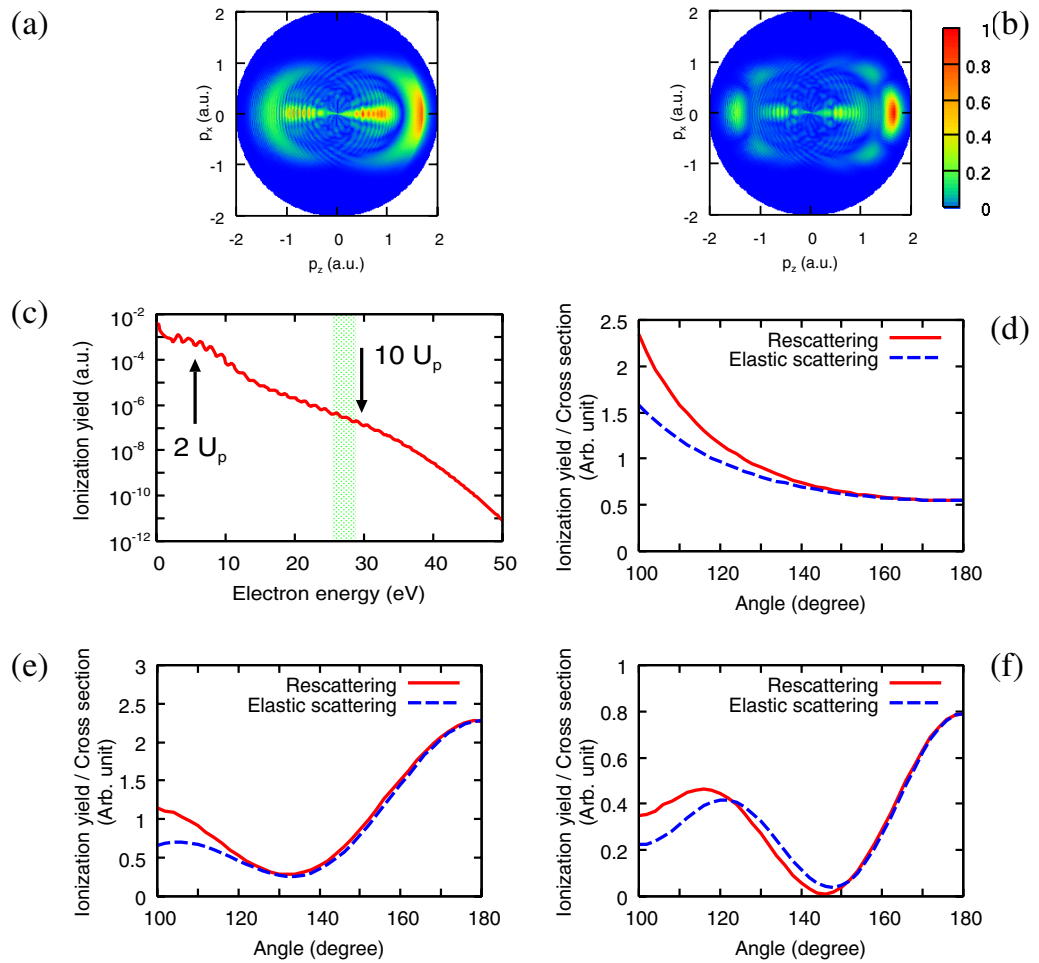
Figure 2. Electron momentum spectra generated by a five-cycle laser pulse, with a peak intensity of $5 \times 10^{13}\,\mathrm{W\,cm^{-2}}$ and a mean wavelength of $800\,\mathrm{nm}$ on the p_z–p_x-plane for (a) H and (b) Xe. The images are renormalized for each photoelectron energy to reveal the global angular distributions. The electron energy distributions for H are shown in (c). The electrons along the BRR are identified by the outermost circular rings on each side. Comparison of the angular distributions of electron images along the BRR with the differential elastic scattering cross-sections by free electrons, (d) H, (e) Ar and (f) Xe, all under the same laser intensity, illustrating that the latter can be extracted from the laser-generated electrons along the BRR. The shift of the center of 0.62 au and the radius of the circle of 0.94 au are used.

'a' and rescattered into the backward directions near 'b' (figure 1(a)). Due to the smaller A_r at 'b', the shift of the center and the radius of the circle are smaller.

Figure 2(b) shows the same normalized momentum images of Xe under the same laser pulse. Here, Xe is treated in the single active electron (SAE) model. Similar shifted half circular rings are seen, but along each BRR, the intensity exhibits a clear dip away from the polarization axis. Can one attribute the difference in Xe and H targets to rescattering alone, i.e. to the difference in the elastic scattering cross-sections by free electrons only?

Taking the *actual* calculated electron yields on the BRR, i.e. along $A_r \hat{p}_z + p_o \hat{p}_r$, we compare the angular dependence of the momentum images on the BRR with the elastic differential cross-sections of Xe^+ with free electrons (figure 2(f)) at incident energy $E_0 = p_0^2/2$, with the scattering angle θ measured from the shifted center. The two curves are in excellent agreement. Similar agreement is shown at the same peak intensity for atomic hydrogen in figure 2(d) and for Ar in figure 2(e). We have also tested other atoms like Ne, and at other intensities and found similar agreement [14]. Similar tests have also been made for atomic negative ions like H^- and F^-, and accurate electron–atom scattering cross-sections are obtained [15].

In calculating the electron-momentum spectra by intense laser pulses, we solved the TDSE of a one-electron model atom in the laser field [16, 17]. Briefly, a model one-electron potential was chosen which reproduces the binding energies of the ground state and the first few excited states of the atom. This same potential is used in the solution of TDSE and in the calculation of the differential elastic scattering cross-sections. The detail of the numerical method used here has been described previously [16, 17]. To obtain accurate results for the high-energy electron momentum spectra near $10\,U_P$ and beyond, care must be taken to ensure that the calculations are converged. In our experience, we have found that discrepancy of the deduced differential cross-sections from laser-induced electron spectra has always been traced to the lack of convergence in the TDSE calculation. A sine-squared pulse with carrier-envelope phase (cep) equal to zero was assumed for all the laser pulses. Since the atomic ions are assumed to be structureless, the differential elastic scattering cross-sections are obtained from the simple potential scattering theory by calculating partial wave phase shifts.

The above results are based on accurate solutions of a one-electron model atom. For most closed-shell atoms, description of one-electron phenomena based on the SAE approximation is quite adequate and is widely used. Since our model does not specifically depend on the one-electron picture, we anticipate that the conclusion would apply to many-electron atoms as well. In such cases, both the laser-induced electron spectra and the elastic scattering cross-sections should be calculated using the many-electron model. While such calculations are widely available for the latter, they are not available for the laser-induced electron spectra at the level of accuracy required here. Existing experimental data also do not have the required accuracy to test the possible many-electron effect in the electron momentum spectra.

We comment that the results shown in figure 2 are from calculations based on a five-cycle pulse with cep $\phi = 0$. For short pulses, it is essential that the cep be stabilized [18]. For a different ϕ, the value of the vector potential at the return time is different and the resulting BRR will be different. For long pulses, electrons born at successive cycles contribute to the momentum spectra, and the yield along the BRR will exhibit interference typical of above-threshold-ionization electrons. In this case, elastic scattering cross-sections can be extracted from the envelope of the electron yield along the BRR. In other words, elastic scattering cross-sections of atomic ions by free electrons can be extracted from rescattering generated photoelectron spectra on the BRR. The extracted cross-sections depend only on the momentum distribution of the returning electron wave packet, independent of the duration, intensity or wavelength of the laser.

3. Implications for molecular targets

Based on the above results which were obtained from 'exact' theoretical calculations, we conclude that laser induced photoelectron momentum images on the BRR allow us to extract
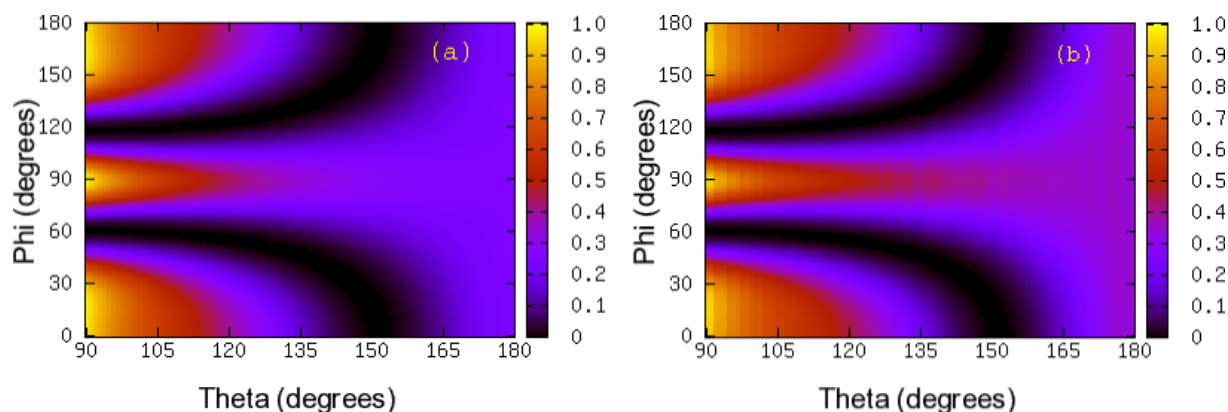
Figure 3. Comparison of (a) elastic differential scattering cross-sections of H_2^+ by electrons with (b) the same information obtained from laser-induced electron images along the BRR, showing good agreement between the two. The molecular axis is perpendicular to the direction of the incident electron, so is the direction of the laser polarization. Electron momentum is $p = 2.2$ au, corresponding to the BRR obtained with a four-cycle laser with peak intensity of $3 \times 10^{14}\,\mathrm{W\,cm^{-2}}$ and a wavelength of 800 nm.

elastic differential scattering cross-sections of the target ion by *free* electrons. While calculations have been carried out only for atoms, we believe that the conclusion can be extended to molecular targets as well. At present, accurate TDSE calculations for the momentum images along the BRR for molecules are not available. Thus we have used the second-order strong field approximation (SFA2) to draw our 'conclusions' for molecular targets. In SFA2, the scattering of the returning electrons with the target ion is treated to first order only. For atomic targets, we have shown [19] that momentum images along the BRR calculated using SFA2 can be used to extract elastic differential cross-sections as well, except that they are calculated within the first Born approximation. Here, we show that first-order elastic differential cross-sections for molecular targets can be extracted from laser-induced electron momentum spectra along the BRR calculated using SFA2. We then extend this to 'conclude' that accurate elastic differential cross-sections can be retrieved for molecular targets as well if accurate photoelectron momentum spectra along the BRR are available from experiments or from accurate TDSE results.

In figure 3(a) we show the differential elastic scattering cross-sections of *free* electrons incident on H_2^+ with the internuclear axis lying perpendicular to the direction of the incident beam. The momentum of the incident electron is 2.2 au, and the internuclear separation of H_2^+ is $R = 3$ au. Taking the incident direction as the z-axis, the differential cross-sections are expressed in terms of spherical angles θ and ϕ, where the former is the polar angle and the latter is the azimuthal angle measured from the molecular axis. In figure 3(b) we show the same elastic scattering cross-sections *derived* from the laser-generated photoelectron momentum spectra along the BRR which is a displaced spherical shell in momentum space with radius 2.2 au. The H_2^+ is in the same geometry. The laser is 5 fs, 800 nm, with peak intensity of $3 \times 10^{14}\,\mathrm{W\,cm^{-2}}$ and polarized along the z-axis. By comparing the two frames, clearly the differential cross-sections extracted from laser-induced photoelectron momentum distributions along the BRR

are in good agreement with the differential elastic scattering cross-sections of the same target ion by *free* electrons.

By taking that accurate differential elastic scattering cross-sections of molecules by free electrons can be extracted from laser induced electron-momentum spectra along the BRR in general, this conclusion has far reaching implications since electron scattering is a powerful tool for determining the structure of molecules in the traditional energy-domain measurements. This implies that infrared lasers can be employed to probe the structure of molecules. For few-cycle infrared lasers, the rescattering of the electrons with the parent ions occurs within the order of 1 fs and with attosecond temporal resolution. Thus few-cycle infrared lasers can handily achieve subfemtosecond temporal resolution, and they may serve as efficient ultrafast cameras for imaging physical, chemical and biological systems where the system is undergoing rapid structural change.

4. Spatial resolution achievable with infrared lasers

Given that elastic scattering cross-sections can be extracted from laser-induced electron momentum spectra, the next question is whether molecular structure can be retrieved with good spatial resolution from these data in view that the energies of the rescattering electrons (of the order of 100 eV or less) are much smaller than those used in the conventional electron diffraction experiments (of the order of 10–100 keV). We think so since in the present scheme electron images are taken only in the backward directions. To make such large angle scattering the electrons have to be scattered from each atomic center in the molecule. The scattered waves from these atomic centers would generate pronounced diffraction images which are to be analyzed to retrieve the positions of the atoms.

Before a retrieval program becomes available, we first show that elastic scattering cross-sections by free electrons (which are to be extracted from laser-induced electron momentum images) are sensitive to the arrangement of atoms in a molecule. These cross-sections can be easily calculated for molecular targets within the first Born approximation. In figure 4, elastic differential cross-sections of H_2^+ at different internuclear distances are shown. The electron momentum is $p = 2.2$ au and the internuclear distances are $R = 2, 3, 4$ and 5 au, respectively. The incident electron beam is perpendicular to the internuclear axis and the spherical angles θ and ϕ are defined as before. One can clearly see that the positions of the interference minima/maxima shift as R increases. Also, as R increases, more interference minima/maxima emerge. In fact, within the first Born approximation, the differential cross-section for this system can be written as

$$\sigma(\theta, \varphi) \sim \cos^2[pR\sin(\theta)\cos(\varphi)].$$

Therefore, destructive interference from the two atomic centers occurs when

$$pR\sin(\theta)\cos(\varphi) = \left(\tfrac{1}{2} + n\right)\pi, \quad n = 0, \pm 1, \pm 2 \dots.$$

The positions of the interference minima shown in figure 4 are in very good agreement with the above equation. Note that the diffraction pattern changes rapidly with respect to R. Thus we anticipate that it would be relatively easy to achieve sub-Angstrom spatial resolution when the internuclear distance is retrieved from these data.

As another example, in figure 5 we show the differential elastic scattering cross-sections from two planar molecules, benzene and nitrobenzene, respectively, with the incident electron
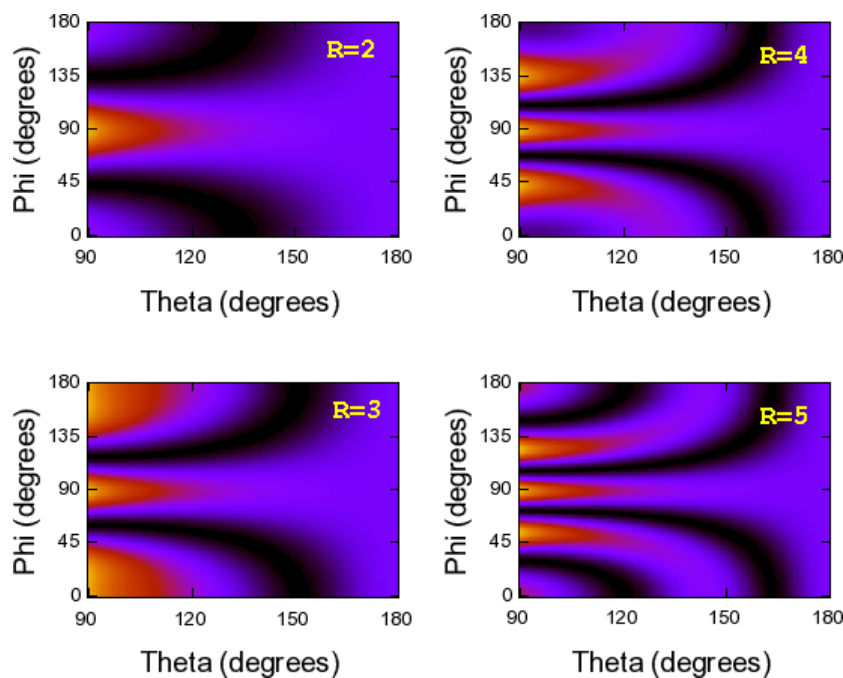
Figure 4. Elastic scattering cross-sections as in figure 3, but at four different internuclear distances.

direction perpendicular to the molecular plane and with momentum at $p = 2.5$ au. The spherical angles are defined as before, with the azimuthal angle ϕ measured from the major symmetry axis of nitrobenzene. From the momentum images, those that are mostly due to the benzene backbone can be identified. Additional features due to the extra nitrogen atoms can also be clearly seen. These two figures show that if only the positions of a few atoms are changed, the diffraction images will also only be modified partially. Such observation will simplify the task of retrieving the structural information on a molecule under transformation since in such transformations often it involves the movement of a few atoms only.

For dynamic chemical imaging, in figure 6, we show how the electron elastic scattering cross-sections (at $p = 2.2$ au) vary as the C_2H_2 molecule goes through intermediate steps in the isomerization process—starting from vinylidene and passing through two transition states TS1 and TS2 and a local minimum M1, and ending up at the global minimum state, acetylene. (For further discussions of these intermediate steps, see [20].) The structural arrangement of the transient molecule at each step is depicted along the left column. The electron momentum images from each configuration show some differences, with the most noticeable difference in vinylidene as compared to acetylene. The images were taken for incident electrons perpendicular to the molecular plane. In this example, the images for the intermediate states do not differ significantly since usually only the light hydrogen atoms undergo position changes. It would be a critical test of the retrieval method in the future to check if such small changes in the images can still be retrieved to obtain accurate molecular structure.

In the above examples, electron momentum images were taken from incident electrons coming from one side only. Consider a moderate-size asymmetric molecule fixed in space. If infrared lasers are used to illuminate this molecule from three perpendicular directions, by
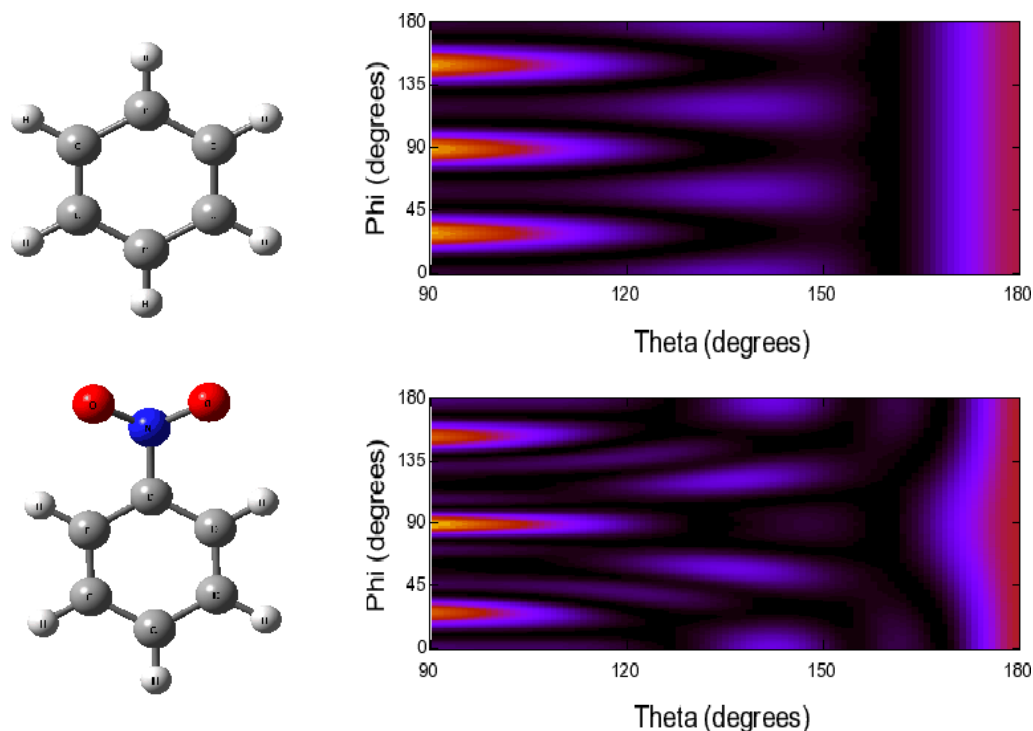
Figure 5. Differential elastic cross-section for electron scattering from benzene (top panel) and nitrobenzene (bottom panel), at the collision momentum of $p = 2.5$ au, as a function of scattering angles θ and φ. The incident beam is perpendicular to the molecular plane in both cases.

collecting momentum images in the backward rescattering directions along each axis, many sets of elastic differential cross-sections can be extracted. Additional data can be obtained from different laser intensities or wavelengths, including lasers with wavelength up to about $2\,\mu$m [21]. A wealth of elastic differential scattering cross-sections would then be available for retrieving the structure of the molecule.

5. Promises and challenges

In this paper, we have shown quantitatively that high-energy electron momentum spectra of a model atom along the BRR induced by few-cycle laser pulses can be used to extract accurate differential elastic scattering cross-sections of the atomic ions by *free* electrons. Since the theory does not rely on whether the target is an atom or a molecule, or whether it is a one-electron system or a many-electron system, we anticipate that the conclusion would apply to molecular targets in general. This generalization is partly supported for molecular targets using the SFA2 theory. These extracted differential cross-sections can in principle be used to retrieve the structure of the molecules. Since the pulse duration of few-cycle infrared pulses is in the order of a few femtoseconds and rescattering occurs within the attosecond scale, we illustrated that such few-cycle infrared laser pulses can be used for dynamic chemical imaging of transient molecules.
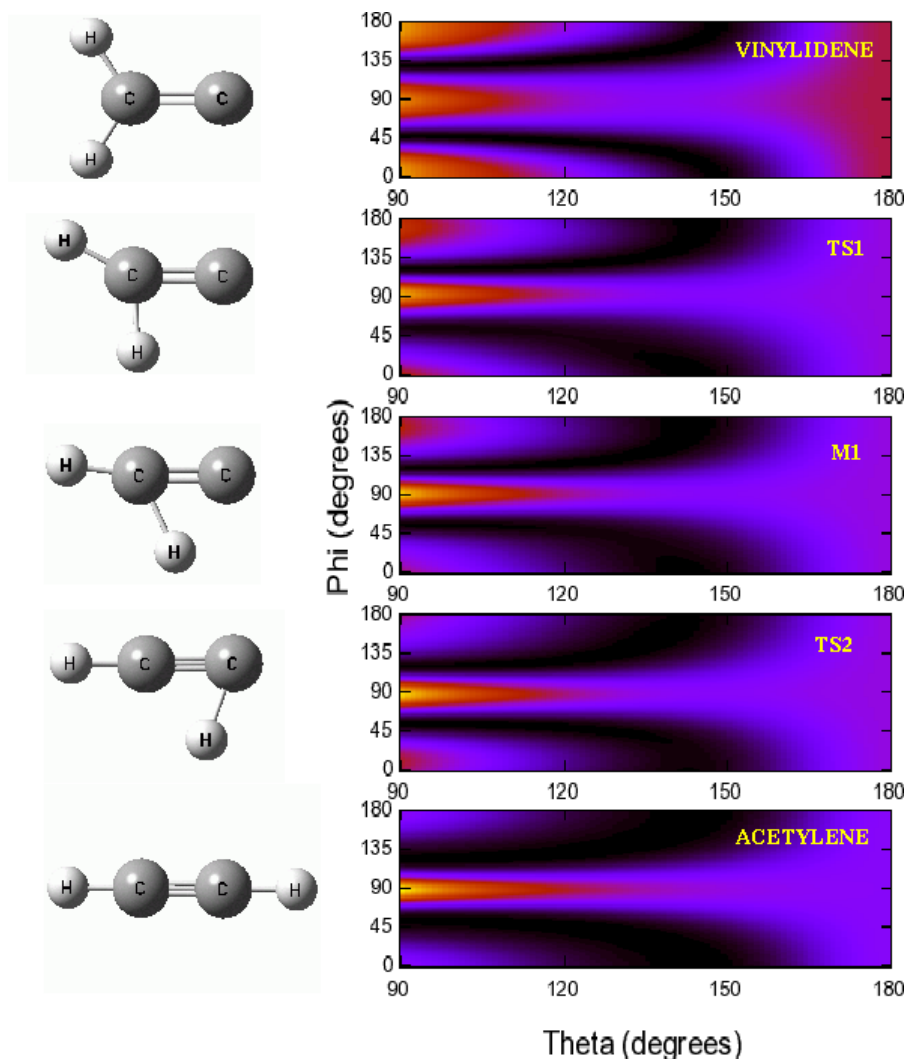
Figure 6. Schematic of dynamical chemical imaging of the isomerization of acetylene/vinylidene using infrared lasers. The isomerization of the linear acetylene molecule (bottom) to the planar vinylidene (top) is assumed to pass through three intermediate/transition states, with their geometries depicted along the left column. For these geometries, the differential elastic scattering cross-sections extracted from the BRR ($p = 2.2$ au) are shown for laser pulses polarized perpendicular to the molecular plane. These images can be used to retrieve the time-dependent structural rearrangement of atoms in the isomerization process.

Experimentally, the momentum spectra on the BRR can be measured with COLTRIMS detectors [22] where momentum images over 4π angles can be collected, or by using time-of-flight methods. Since the yields of high-energy electrons on the BRR are small, one may want to enhance counting rates by increasing gas pressure, by increasing the repetition rates of the laser pulses, or by increasing laser intensities. In the future, one may want to look into other optical methods, such as superposing attosecond pulse trains [23], to enhance the yield of the returning electrons and to increase the electron counts on the BRR.

The calculations presented so far are for molecules fixed in space. For molecules in the gas phase, they are isotropically distributed initially. To retrieve structural information, they should be at least partially aligned before electron spectra are taken. Molecules can be partially aligned in 1D with one laser or in 2D or 3D with two or more lasers [24, 25]. The degree of alignment of small molecules can be measured by Coulomb explosion independently, or calculated theoretically [24]. If the molecules are not aligned then partial information, such as the internuclear separation, may still be extracted (but not the bond angles), as has often been done in electron diffraction experiments [26].

To image the dynamic evolution of the structural change of a molecule, a pump–probe scheme will be used. A pump pulse creates a molecular wave packet, and the time evolution of this wave packet, in particular the coordinates of the atoms, are to be retrieved from the probe pulse measurements at different time delays, thus to create a molecular movie where the chemical transformation can be followed in femtosecond timescale.

Clearly, many experimental and theoretical issues remain to be worked out for LIEM to become a reality. Here we just mention two. (i) Calculation of accurate elastic scattering cross-sections by free electrons from molecular ions. To begin with, such calculations are needed to test how much the diffraction images as shown in figures 3–6 are modified in a real situation. Fortunately, computer codes for such calculations are already available [27]–[30]. For specific molecules, many-electron effects can also be incorporated in principle but will be quite tedious. It remains to be seen whether high-precision electron scattering data are needed for the determination of the structure of molecules at the level of finding the temporal positions of all the atoms. (ii) The possible breakdown of the present model for polyatomic molecules. It may be argued that the binding energies of polyatomic molecules are usually smaller and many-electron effects are important such that the present model would fail. Unless proved otherwise experimentally, at this time we still believe the model will work. The model relies on the back scattering of the target ion by an electron wave packet generated by tunnel-ionization of the molecule. For polyatomic molecules, one may want to use lasers of longer wavelength such that ionization is initiated by tunneling. For negative atomic ions which have low binding energies, we have shown from TDSE calculations that the present model works well when lasers with longer wavelengths are used. When many-electron effect becomes important for polyatomic molecules under transformation, one can still extract elastic scattering cross-sections by free electrons from the laser-induced electron spectra along the BRR, and the spectra would reflect the change of the geometry of the polyatomic molecules with time. Since the change of correlation energy (or effect) is expected to be less important than the change of electrostatic energy due to the change of the geometry of a molecule, we believe partial information on the structural change of the molecule can still be extracted using the LIEM method even if the many-electron effect is large. On the other hand, for the LIEM method to become a reality, experimental progress is urgently needed. At this time, even data for atomic targets would be very valuable, to demonstrate that elastic scattering cross-sections can indeed be extracted from the BRR and they can be compared to data generated from electron scattering experiments directly.

Acknowledgments

References

[1] Fienup J R 1982 *Appl. Opt.* **21** 2758–69

[2] Miao J, Charalambous C, Kirz H and Sayre D 1999 *Nature* **400** 342–4

[3] Ihee H, Lobastov V A, Gomez U M, Goodson B M, Srinivasan R, Ruan C Y and Zewail A H 2001 *Science* **291** 458–62

[4] Grinolds M S, Lobastov V A, Weissenrieder J and Zewail A H 2006 *Proc. Natl Acad. Sci. USA* **103** 18427–31

[5] Baum P and Zewail A H 2006 *Proc. Natl Acad. Sci. USA* **103** 16105–10

[6] Gedik N, Yang D S, Logvenov G, Bozovic and Zewail A H 2007 *Science* **316** 425–9

[7] Zou T, Bandrauk A D and Corkum P B 1996 *Chem. Phys. Lett.* **259** 313–20

[8] Lein M, Marangos J P and Knight P L 2002 *Phys. Rev.* A **66** 051404

[9] Hu S X and Collins L A 2005 *Phys. Rev. Lett.* **94** 073004

[10] Spanner M, Smirnova O, Corkum P B and Ivanov M 2004 *J. Phys. B: At. Mol. Opt. Phys.* **37** L243–50

[11] Yurchenko S N, Patchkovskii S, Litvinyuk I V, Corkum P B and Yudin G L 2004 *Phys. Rev. Lett.* **93** 223003

[12] Paulus G G, Becker W, Nicklich W and Walther H 1994 *J. Phys. B: At. Mol. Opt. Phys.* **27** L703–8

[13] Yang B, Schafer K J, Walker B, Kulander K, Agostini P and DiMauro L F 1993 *Phys. Rev. Lett.* **71** 3770–3

[14] Morishita T, Chen Z J, Le A T and Lin C D *Phys. Rev. Lett.* accepted

[15] Zhou X X, Chen Z J, Morishita T, Le A T and Lin C D 2007 *Phys. Rev.* A submitted

[16] Chen Z, Morishita T, Le A T, Wickenhauser M, Tong X M and Lin C D 2006 *Phys. Rev.* A **74** 053405

[17] Morishita T, Chen Z, Watanabe S and Lin C D 2007 *Phys. Rev.* A **75** 023407

[18] Baltuska A *et al* 2003 *Nature* **421** 611–5

[19] Chen Z, Morishita T, Le A T and Lin C D 2007 *Phys. Rev.* A **76** 043402

[20] Le V H, Le A T, Xie R H and Lin C D 2007 *Phys. Rev.* A **76** 013414

[21] Fuji T, Ishii N, Teisset C Y, Gu X, Metzger T, Baltuska A, Forget N, Kaplan D, Galvanauskas A and Krausz F 2006 *Opt. Lett.* **31** 1103–10

[22] Ullrich J, Moshammer R, Dorn A, Doerner R, Schmidt L P H and Schmidt-Boecking H 2003 *Rep. Prog. Phys.* **66** 1463–545

[23] Schafer K J, Gaarde M B, Heinrich A, Biegert J and Keller U 2006 *Phys. Rev. Lett.* **92** 023003

[24] Stapelfeldt H and Seidemann T 2003 *Rev. Mod. Phys.* **75** 543–57

[25] Lee K F, Villeneuve D M, Corkum P B, Stolow A and Underwood J G 2006 *Phys. Rev. Lett.* **97** 173001

[26] Hargittai I and Hargittai M 1988 *Stereochemical Applications of Gas-Phase Electron Diffraction* (New York: VCH)

[27] Tonzani S 2007 *Comput. Phys. Commun.* **176** 146

[28] Tonzani S and Greene C H 2006 *J. Chem. Phys.* **124** 054312

[29] Liu X J, Lucchese R R, Grum-Grzhimailo A N, Morishita Y, Saito N, Prumper G and Ueda K 2007 *J. Phys. B: At. Mol. Opt. Phys.* **40** 485–96

[30] Toffoli D, Lucchese R R, Lebech M, Houver J C and Dowek D 2007 *J. Chem. Phys.* **126** 054307